Gu C, **Anderson, William**, F Maggi (2012) Riparian biogeochemical hot moments induced by stream fluctuations, Water Resour Res 48:W09546, doi:10.1029/2011WR011720. Version of record available from Wiley [ISSN: 0043-1397], [DOI: 10.1029/2011WR011720]

Riparian biogeochemical hot moments induced by stream fluctuations

[1] Hyporheic exchanges in riparian zones induced by stream stage fluctuations, referred to as bank storage, can influence contaminant transport and transformation when mixing of groundwater and surface waters with distinct chemical signatures occur, which might lead to a high biochemical activity. The effect of bank storage on nutrient transport was analyzed here using a two-dimensional, variably saturated and multispecies reactive transport model, which accounted for the water flow and solute transport and reactions within riparian zones. After verification with field observations, our model demonstrated that high biogeochemical activities occurred at the near-stream riparian zone during stage fluctuation, a process referred to as bank storage hot moment (BSHM). We used Monte Carlo simulations to study the uncertainty of BSHM and related nutrient dynamics to biogeochemical and hydrological factors. The results indicated that stream fluctuations can lead to maximum bank storage volume ranging from 0 to 259 $m^3\ m^{-1}$ of stream linear length (median = 9.7 m^3 and SD = 53.2 m^3). Taking denitrification as an example, BSHM can lead to considerable NO_3^- removal with a median removal rate of 2.1 g d^{-1} and SD of 17.2 g d^{-1} per meter of stream linear length. The NO_3^- uptake velocity (median = 2.7×10^{-5} and SD = 2.4×10^{-4} m min^{-1}) was comparable to that of in-stream transient storage from the literature. This result suggests that BSHM may be a significant process contributing to the nutrient budget at the ecosystem level. Finally, a theoretical framework representing the coupled hydrobiogeochemical controls on riparian hot spots was developed to help predicting when BSHM can become important in a particular stream.

1. Introduction

[2] Riparian zones are the interface of terrestrial and aquatic ecosystems, where water from various sources meet and lead to dynamical hydrological and biogeochemi-cal processes [*Hill*, 1996; *Vidon et al.*, 2010]. The variabili-ty and heteorogeneity of soil water content, redox potential, and substrate supply can contribute to the biogeochemical activity and the exchange rate of chemicals from upland to stream, and vice versa [*Hedin et al.*, 1998; *McClain et al.*, 2003; *Vidon and Hill*, 2004a]. Understanding solute dynamics under variable hydrological conditions is fundamental to quantifying solute loads to surface waters given that a large fraction of the annual solute fluxes are mainly associated with hydrological events [*Boyer et al.*, 1997]. There have been many studies of the roles of the riparian zone in controlling runoff and associated solute transport [*Hornberger et al.*, 1994; *Inamdar and Mitchell*, 2006; *McGlynn and McDonnell*, 2003], but very few have focused on the impact of lateral stream-riparian interaction induced by hydrological events on solute transport. Since riparian zones are the direct interface between different waters and play a critical role in controlling chemical transport [*Chanat and Hornberger*, 2003], a thorough understanding of solute transport through riparian zones must be framed within a stream-aquifer continuum modeling approach [*Allan et al.*, 2008; *Hill et al.*, 2000]. Emphasis is given here to identifying the location, timing, and duration of these biogeochemical reactions.

[3] Large-scale hyporheic exchange in the riparian zone are referred to here as bank storage to be distinct from in-stream hyporheic exchange [*Cooper and Rorabaugh*, 1963]. Both riparian and in-stream hyporheic exchanges are restricted by regional groundwater discharge in base flow conditions [*Boano et al.*, 2008; *Cardenas and Wilson*, 2006]. The riparian hyporheic exchange, however, can be enhanced by stream stage fluctuations caused by hydrological perturbations such as floods [*Bates et al.*, 2000], reservoir releases [*Sawyer et al.*, 2009], and snowmelt [*Loheide and Lundquist*, 2009]. These transient conditions can lead to the dynamic development of the hyporheic zone [*Gerecht et al.*, 2011]. In turn, the extent of the hyporheic zone can affect the stream and riparian water chemistry [*Valett et al.*, 1996]. The exchanges through the riparian zone bring surface water rich in oxygen (O_2) and organic matter (OM) into the riparian

zone through groundwater recharge by infiltration and then return mixed stream and groundwater back to the surface water through groundwater discharge [*Findlay*, 1995]. In a study of riparian hyporheic exchange impacted by dam operation, *Sawyer et al.*, [2009] found that riparian water chemistry and temperatures fluctuated in response to the flow regime. A recent study in an urban stream subject to summer thermal fluctuations suggested that bank storage can serve as a thermal sink to mitigate temperature surges [*Anderson et al.*, 2011]. Ground- and surface water mixing caused by bank storage has legacy effects on contaminant flux through the hyporheic zone [*Fritz and Arntzen*, 2007], thus affecting the chemical signature of groundwater discharge used in chemical hydrograph separation [*McCallum et al.*, 2010]. Studies have shown that such two-way exchange can impact riparian and stream chemistry as long as several weeks after floodwaters recede [*Baillie et al.*, 2007; *Squillace*, 1996]. However, none of these studies has investigated the potential significance of bank storage on riparian biogeochemistry and riverine chemical budget across a wide spectrum of field conditions. We attempted to fill this knowledge gap using a theoretical framework in this study.

[4] Mixing of groundwater with geochemically contrasting surface waters can create an important biogeochemical hot moment in the near stream-riparian areas, which can alter the geochemical conditions along the discharge pathway [*Findlay*, 1995]. Although changes in redox conditions can affect several oxic and anoxic biogeochemical processes in a transient manner, these can result in persistent and significant effects on the nutrient distribution in the near-stream groundwater and subsequent efflux to surface waters. For example, O_2 intrusion into the riverbed can create oxic conditions within the hyporheic sediment [*Baker et al.*, 1999]. In these cases, O_2 would presumably be consumed during microbial heterotrophic respiration, and could alter the stream O_2 budget [*Findlay*, 1995]. Hydrologically regulated redox conditions are also important for the nitrogen cycling [*Cirmo and McDonnell*, 1997]. Denitrification hotspots are often found in concomitance with low dissolved O_2 and available organic carbon (OC) and NO_3^- [*McClain et al.*, 2003]. For example, *Devito et al.* [2000] showed that downward hydrologic gradients created by microtopography can facilitate OC transport from surface peat layers to underlying carbon-depleted sandy sediments, thus providing the electron donor required for denitrification. Sustained bank filtration in low gradient streams was found to be a hot spot of NO_3^- removal in riparian zones [*Duval and Hill*, 2007]. Hyporheic flow can contribute to removing NO_3^- from the stream by delivering it into the anaerobic subsurface where denitrification occurs [*Kasahara and Hill*, 2006]. The interaction between OC supply, N and O_2 availability, as well as other biogeochemical reactions make bank storage processes at near-stream-riparian zones a hot moment with regards to the overall chemicals budget and turnover time [*Rassam et al.*, 2006]. It remains challenging to understand where, when, and how bank storage regulates solute transport and loads to stream ecosystems.

[5] The main goal of this work was to identify the effects of the bank storage on riverine contaminant transport using a variably saturated flow and multispecies reactive transport model. This model was first tested against the field observation at a 53 m wide floodplain site on the South Fork New River, NC, where piezometric heads, river stage, and water temperature were available to validate the hydraulic transport components of the model. This model was then used to simulate riparian biogeochemistry using a reactive transport module. The redox condition in the riparian zone was accounted for by tracking O_2 dynamics explicitly. Simulations with stream stage fluctuation were presented to illustrate its effects on the spatial and temporal extent of a biogeochemical hot spot in riparian zones and thus contaminant flux across the stream-aquifer interface. The sensitivity of BSHM and related nutrient dynamics to biogeochemical and hydrological factors were analyzed using Monte Carlo simulations. Finally, we compared the storage and nutrient uptake metrics of BSHM with those of well-studied in-stream transient storage process. A significance index representing the coupled hydrobiogeochemical controls on riparian hot spots was developed to help predicting when BSHM can become important in a particular stream.

2. Methods

2.1. Study Site

[6] The field investigation is carried out in the South Fork New River (SFNR), North Carolina (NC), USA (Figure 1). The 80 km^2 SFNR watershed is located in the

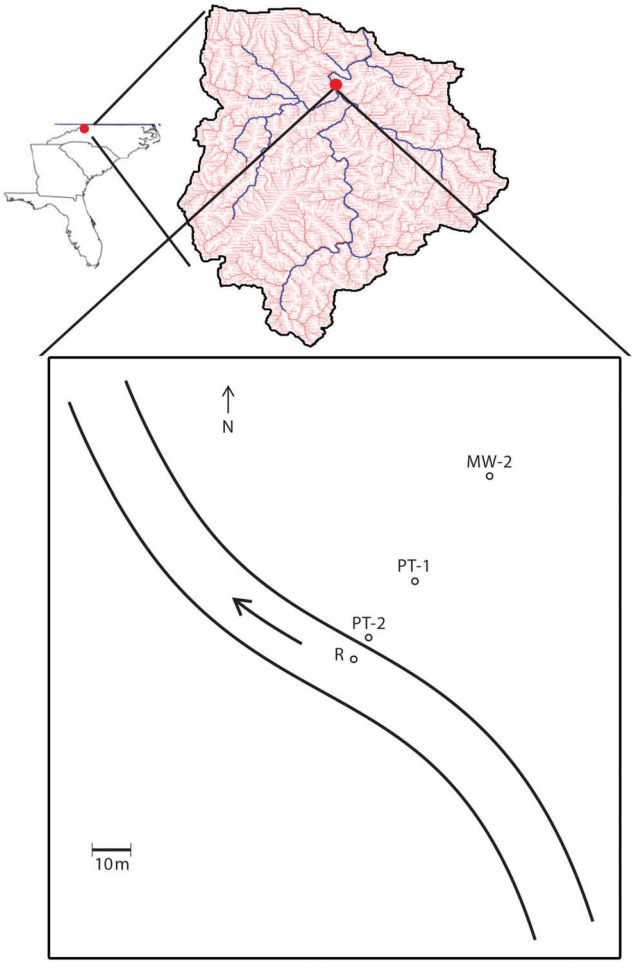

Figure 1. Site map of the South Fork New River watershed, showing the locations of the monitoring wells.

Blue Ridge province, an area characterized by rugged, mountainous terrain with an average slope of 27%. Hydrologic investigations were initiated at a floodplain aquifer immediately adjacent to the SFNR in Spring 2010. The SFNR flowing through the study site is incised to a depth of approximately 3 m into the floodplain.

[7] The site is subject to substantial flood inundations about three or four times per year. The site is constrained by a hillslope approximately 53 m upland. A series of eight monitoring wells were installed, including a transect of wells perpendicular to the river that included MW-2 well near the edge of foothill, through PT-1 well, to PT-2 well. The MW-2, PT-1, and PT-2 wells were located about 50, 20, and 2 m from the river bank, respectively (Figure 2). Water levels and temperature were recorded in the PT-2 well at 10-min intervals with pressure transducers. The river stage was measured at 10-min intervals with a water level logger. The preliminary well log and geophysical survey data showed evidence of development of alluvial geomorphology. The floodplain aquifer at the study site, especially near the river, consisted of a silty topsoil 1 m thick underlain by about 3 m thick coarse-grained alluvium, and finer sediments beneath. The average aquifer depth is about 5 m, determined by both the well logs and direct current resistivity surveys [*Bailey et al.*, 2010].

2.2. Modeling

[8] A two-dimensional finite element flow and transport model was developed to describe water and solute exchanges induced by bank storage [*Gu et al.*, 2008b]. The model simulated variably saturated flows by solving the two-dimensional mixed-form Richards equation. We specifically included a sloping bank instead of a vertical bank for the riparian-stream interface. Our approach overcomes earlier assumptions such as fully penetrating streams, vertical river banks, and fully saturated flow [*Boutt and Fleming*, 2009; *Chen and Chen*, 2003; *Whiting and Pomeranets*, 1997]. These assumptions are rarely met in reality and can lead to erroneous results of stream-aquifer exchanges [*Doble et al.*, 2012]. Additionally, the model accounted for reactive advective-dispersive transport processes based on the transient hydraulic head distribution and corresponding velocity field calculated from the flow model [see *Gu et al.*, 2008a for details].

2.2.1. Field and Modeling Characteristics

[9] The model domain (Figure 1) is a vertical cross section 53 m wide and 7 m deep through the floodplain between the hillslope (left) and the river channel (right). The domain is described by two hydrostratigraphic units as reported in *Bailey et al.* [2010]. Unit 1 is designated as coarse-grained alluvial deposits. Unit 2 is represented by fine silt. A saturated hydraulic conductivity of 10 and 1 m d^{-1} were assigned to unit 1 and unit 2, respectively, after field pumping tests. A Dirichlet (constant head) boundary condition was assigned to the landward vertical upslope shoulder of the hillslope. A time varying specific head boundary was assigned along the river channel grids below the river stage using observed river stage hydrograph data. The river channel represents half the channel width, with zero-flow boundary assigned along the vertical boundary at the center of the river channel. The low-permeability aquitard at the bottom of the domain was also treated as a zero-flow boundary. The upper atmospheric boundary accounted for evapotranspiration and groundwater recharge. We simply applied a constant water influx of 0.002 m d^{-1} to represent groundwater recharge from precipitation for the duration of each simulation. The discretization was nonuniform with finer grids toward the stream-riparian interface. The area adjacent to the river channel was discretized to 0.1 m horizontally and 0.1 m vertically.

[10] A seepage face was simulated at the stream-aquifer interface, where water leaves the saturated zone freely and the pressure head is uniformly zero. Since the length of the seepage face was not known beforehand, iterations were required to constantly adjust the span of seepage face. The location of the seepage face required a check on the Darcy flux, which was computed by taking the derivatives of the computed pressure head over the boundary elements. At nodes where the pressure head was negative, a Neumann boundary (i.e., zero flow) was assigned. At the nodes with outward fluxes, a Dirichlet boundary (i.e., zero pressure head) was specified as by *Cooley* [1983].

[11] The initial hydraulic head was generated by running a transient model with constant boundary conditions at the

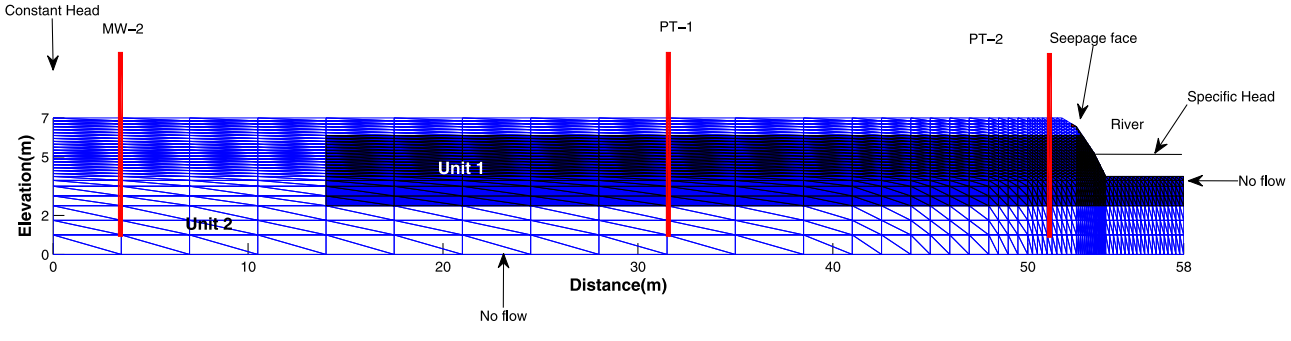

Figure 2. Finite element meshes and boundary conditions constructed for the hillslope-riparian transect. The mesh consists of 2226 nodes and 4256 linear, triangular finite elements. Layer shading indicates specific hydrostratigraphic units for hydraulic flow model of stream stage fluctuation. Hydraulic head observation well PT-1, PT-2, and MW-2 are marked with solid lines. The flow boundaries are also labeled.

hillslope boundary and river stage. A time step $\Delta t = 1$ h ensured numerical stability against Courant condition. The unsaturated soil hydraulic conductivity was accounted for using the Brooks and Corey soil water retention model [*Brooks and Corey*, 1966]. The residual and saturated moisture contents and the Brooks and Corey parameters were determined from in situ soil characteristics (Table 1).

2.2.2. Solute Transport Model

[12] The transport module solved the advection-dispersion equation based on the velocity fields generated from the flow model. A Dirichlet boundary condition was applied to the left boundary and top boundary to represent constant chemical source from upland areas and recharge, respectively. A Cauchy boundary condition was applied to the bottom and right boundaries. When the water flux was toward the riparian aquifer, a Dirichlet boundary was applied to the chemical influx from stream water. The Dirichlet boundary condition allowed mass to enter the model domain by both advection and dispersion. When the water flux was from the riparian zone to the stream, the Dirichlet boundary was replaced by Cauchy boundary (i.e., only advection).

Table 1. Hydraulic and Kinetic Parameters for the Baseline Simulation and Monte Carlo Simulations

Parameter	Value[a]	Range
Chemical and Kinetic Parameters		
O_2 Concentration in the Stream (mg L^{-1})	8	
DOC Concentration in the Stream (mg C L^{-1})	15	0.1–25
NO_3^- Concentration in the Stream (mg N L^{-1})	10	0.1–25
O_2, NO_3^-, and DOC Concentration in the Aquifer and Recharge Water (mg L^{-1})	0	
μ, Specific Maximum Aerobic Respiration Rate (mg L^{-1} d^{-1})[b]	3	0.3–30
μ, Specific Maximum Denitrification Rate (mg L^{-1} d^{-1})[b,c]	1	0.1–10
K_a, Half Saturation Constant for O_2 (mg L^{-1})[b,d–f]	1	
K_a, Half Saturation Constant for NO_3^- (mg L^{-1})[b,d–f]	1	
K_d, Half Saturation Constant for DOC (mg L^{-1})[b,d–f]	2	
K_I, Oxygen Inhibition Constant on Denitrification (mg L^{-1})[d,e,g]	1	
Physical and Hydraulic Parameters		
Residual Water Saturation[h]	0.1	
Brooks and Corey Empirical Parameter a[h]	10	
Brooks and Corey Empirical Parameter c[h]	4	
Brooks and Corey Empirical Parameter d[h]	2	
K_s, Saturated Hydraulic Conductivity (m d^{-1})[i]	5	0.1–100
Anisotropy Ratio (–)[i]	0.2	0.1–1
Hydraulic Gradient (–)	0.01	0.001–0.016
α_L, Longitudinal Dispersivity (m)[j,k]	1	0.5–5
α_T/α_L, Transverse/Longitudinal Dispersivity Ratio[i]	0.1	
Specific Yield (–)[h]	0.27	
Hydrograph Peak (m)[h]	1	0.2–2
Hydrograph Duration (day)[h]	3	1–7

[a]The baseline value is either from the field observation or a median value of all data from the literature.
[b][*Gu et al.*, 2007; *Lee* et al., 2006; *MacQuarrie et al.*, 2001].
[c][*Hanson et al.*, 1994; *Kaushal et al.*, 2008; *Pinay et al.*, 1993.
[d][*Kindred and Celia*, 1989].
[e][*Chen et al.*, 1992].
[f][*Doussan et al.*, 1997].
[g][*Tiedje*, 1988].
[h]The field observation in this study.
[i][*Fetter*, 2001].
[j][*Gelhar et al.*, 1992].
[k][*Neuman*, 1990].

2.2.3. Biogeochemical Model

[13] The riparian aquifer acts as a transitional zone between two chemically distinct waters, namely stream water and groundwater. Stream water is usually rich in O_2, dissolved organic carbon (DOC), and nutrients, whereas groundwater is characterized by low DOC concentrations [*Dahm et al.*, 1998]. Microbial biomass metabolic rates in the riparian zone are largely controlled by the DOC [*Baker et al.*, 2000].

[14] Here, O_2, NO_3^-, and DOC were used as three chemical species to track the riparian biogeochemical process. We assumed that groundwater was depleted in NO_3^- and DOC and the absence of DOC at depth is often cited as the limiting control on denitrification in subsurface sediments [*Cey et al.*, 1999; *Gold et al.*, 2001]. On the other hand, the stream water was assumed to have varying NO_3^- and DOC concentration. Sources of stream DOC can be attributed to algae or leaf litter decomposition [*Schlesinger*, 1997]. This study did not consider DOC leaching from OM-rich shallow soils and riverbeds for simplicity. In fact, this process is kinetic controlled and would provide a more enhanced and continuous C source than the stream water itself [*Gu et al.*, 2007]. As a result, this study provided only a conservative estimate of DOC influx from the stream infiltration.

[15] Throughout the streamlines in the aquifer, O_2 was utilized by aerobic respiration as

$$CH_2O + O_2 \rightarrow H_2O + CO_2. \quad (1)$$

[16] And after O_2 was depleted, NO_3^- was consumed as an alternative electron acceptor during denitrification as

$$1.25CH_2O + NO_3^- + H^+ \rightarrow 0.5N_2 + 1.75H_2O + 1.25CO_2. \quad (2)$$

[17] Multiple Monod kinetics was used to describe the above reactions:

$$R_i = \frac{v_{\max i} X_i a_i}{K_{ai} + a_i} \frac{d_i}{K_{di} + d_i} I_i S = \frac{\mu_i a_i}{K_{ai} + a_i} \frac{d_i}{K_{di} + d_i} I_i S, \quad (3)$$

where i is the generic reaction index (i.e., aerobic respiration and denitrification), R_i is the reaction rate (mg $L^{-1}d^{-1}$), μ_i are the lumped specific maximum microbial reaction rates (mg $L^{-1}d^{-1}$) [$\mu_i = v_{\max i} X_i$, $v_{\max i}$ is the asymptotic maximum specific uptake rate of microbial reactions (d^{-1}), X_i is the biomass concentration of aerobe and denitrifier (mg L^{-1})], a_i (mg L^{-1}) is the electron acceptor concentration (mg L^{-1}), d_i is the electron donor concentration (mg L^{-1}), K_{ai} is the half-saturation constant for electron acceptors (mg L^{-1}), and K_{di} is the half-saturation constant for electron donors (mg L^{-1}). The O_2 inhibition of denitrification was modeled through the inhibition factor I_i, given by $I_i = K_{Ii}/(K_{Ii} + a_o)$, where a_o is the inhibitor (i.e., O_2) concentration (mg L^{-1}), and K_{Ii} is the inhibition constant (mg L^{-1}). S is the soil water saturation. We modeled inhibited denitrification in aerated unsaturated soil using a linear proportionality with the water saturation S in Eq. (3). I_i and S are absent in Eq. (3) for aerobic respiration.The model did

not explicitly describe the microbial biomass dynamics so that μ is a constant.

[18] O_2, DOC, and NO_3^- consumption rate were calculated by multiplying R_i by O_2, DOC, and NO_3^- stoichiometric coefficient v_i as

$$\frac{dc_i}{dt} = R_i v_i. \tag{4}$$

[19] The kinetic rate constants and boundary conditions of solute transport are listed in Table 1.

2.2.4. Quantification of Biogeochemical Reaction and Hydrological Exchange

[20] To quantify the magnitude of denitrification rate in the riparian zone throughout the bank storage, the total NO_3^- mass M removed during the stream fluctuations was calculated by

$$M = \int_0^T \sum_e \int_{\Omega_e} \theta \times R d\Omega dT, \tag{5}$$

where θ is the volumetric water content, R is as in Eq. (3), e is the grid element, Ω is modeling domain, Ω_e is the domain occupied by element e, and T is total simulation time.

[21] The instantaneous volumetric flow rate Q across the river-riparian interface per unit length of river is calculated using the Darcy's law:

$$Q(t) = \int_l K \times i(l,t) dl, \tag{6}$$

where K is the hydraulic conductivity of the sediments adjacent to the river, i is the hydraulic gradient along the river channel, and l is the length of the river-riparian interface. Positive values indicate flow from the river into the riparian zone and negative values indicate flow into the river.

[22] Bank storage volume $V(t)$ is defined as the cumulative discharge of water per unit length of river that has entered the riparian from one side of the river over time t, and was calculated by integrating Q along the river-riparian interface during both inflow and return flow as

$$V(t) = \int_0^t Q(t) dt. \tag{7}$$

[23] The maximum bank storage volume ($V_{\max}$) of stream water was estimated as the maximum value of V calculated in Eq. (7). The time from the start of losing stream conditions to the end of the return flow of bank storage water (i.e., when bank storage approaches zero) is the time period when bank storage water is present, and is defined as the hyporheic exchange time.

[24] A conservative tracer was used to determine the hyporheic zone defined as the volume of sediment containing at least 10% river water [*Triska et al.*, 1989]. We then used the tracer concentration contour line of 1/10th of its concentration in the river to delineate the hyporheic zone according to the mixing equation

$$C = C_g(1 - w) + C_s w, \tag{8}$$

where w is the mixing ratio ($w = 0.1$ in this case), C_g is the tracer background concentration in groundwater, C_s is the tracer concentration in river water, and C is the tracer concentration in groundwater after the mixing.

2.2.5. Monte Carlo Simulation

[25] To study the uncertainty of the magnitude of BSHM as well as the impact of hydrological variables on BSHM, a Monte Carlo analysis was performed for the riparian zone and processes described above. The baseline simulation was obtained using the parameters seen in the literature (Table 1). We expanded the model domain length to 100 m to minimize the upland boundary effect and assumed a homogeneous aquifer for simplicity. We applied varying regional groundwater hydraulic gradients to study the impact of landscape topography on the BSHM (i.e., high-relief floodplains versus low-relief floodplains). For the baseline model, the streamside flood pulse was defined using a specified head boundary applied to model grids along the stream-aquifer interface below the varying stream stages, which was represented by an arbitrary stream stage hydrograph. We took a fixed shape of the flood peak by assuming that the time of the flood peak is [1/4] of the duration of the flood wave. According to *Cooper and Rorabaugh* [1963], the hydrographs $H(t)$ under these assumptions can be approximated as

$$H(t) = N h_0 e^{-\omega t}(1 - \cos \omega t), \quad 0 \le t \le \tau, \tag{9}$$

where h_0 is the maximum stage rise, t is the time since the beginning of the flood, τ is the duration of the flood, $\omega = 2\pi/\tau$, and $N = 1/e^{-\pi/2}$ is a constant that scales all the hydrograph peaks to the same height h_0 regardless of the storm duration.

[26] Latin-hypercube sampling (LHS) was used to generate the multivariate parameter distributions for the Monte Carlo simulations. LHS is a type of stratified sampling that reduces the number necessary for a Monte Carlo simulation. Nine variables were considered in the Monte Carlo analysis and a sample size of $N = 200$ was assumed to be sufficiently large [*Iman and Helton*, 1988]. The physical and biogeochemical parameters for the Monte Carlo simulation are summarized in Table 1. Values of the nine parameters were selected from uniform random distributions with the bounds being the parameter ranges typical of stream-riparian zones found in literature. The model output variables included the maximum bank storage volume $V_{\max}$, the exchange time t, and total mass removal M.

3. Results

3.1. Model Test

[27] The flow and transport components of the model were validated against the water table and temperature data collected at the site. The modeled water flows and temperature dynamics were validated by comparison with observed hydraulic heads and water temperature at the observation well PT-2 during and after a precipitation event on 17 August 2010 (Figure 3). Generally, the timing and magnitude of the modeled hydraulic heads and water temperature compared well with the observations, except for the late part of the recession curves. The coefficient of determination R^2 between the observed and modeled water table and

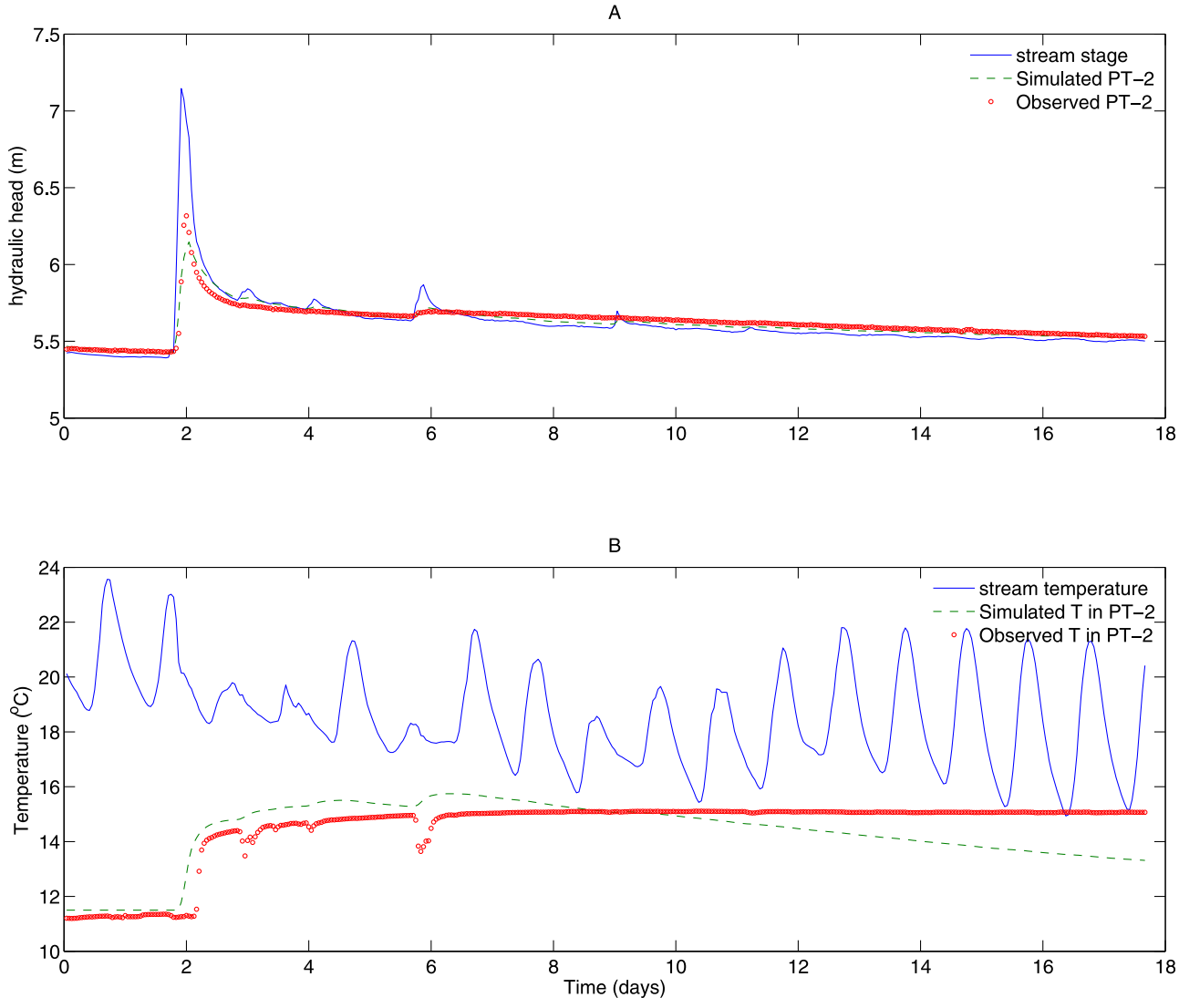

Figure 3. Comparison between observed and simulated (a) water table and (b) water temperature dynamics during a rainfall event on 17 August 2010 using the heat capacity of water C_w, 4.182 × 10^6 J/(m^3 °C), the heat capacity of the saturated streambed C_m, 2.516 × 10^6 J/(m^3 °C), and the thermal conductivity of the saturated sediment k_T, 1.67 J/(s m °C) [*Anderson et al.*, 2011].

temperature were 0.73 and 0.67, respectively. The head gradient reversals during the precipitation indicated a change of flow direction from a gaining river to a losing river as the stage arose. The infiltration of warmer river water caused abrupt water temperature rise in the PT-2 well. The water temperature in PT-2 stayed high and gradually decreased over the long recession period.

3.2. Exemplifying Simulation: Single Storm Event

3.2.1. Flow Pattern

[28] In the baseline simulation, the stage fluctuation caused hydraulic head redistribution in the near-stream riparian zone as compared to steady state conditions prior to the stage fluctuation (Figure 4). The maximum Darcy velocity occurred at the intersection of the water table and the seepage face. A majority of groundwater seepage occurred along the stream bank as horizontal flow because of anisotropic K (i.e., low vertical K). The flow vectors indicate a strong influx of stream water (long arrows and the closely spaced hydraulic head contour) into both the unsaturated and saturated riparian zones at t = 1 day, when the stream stage reached its maximum level (see Figure 3 for the constructed stream hydrograph). The water table hinged around the stream bank, resulting in a reversal of the hydraulic gradient (i.e., landward gradient). Right after the stage peak passed after time t = 3 day, the streamward hydraulic gradient recovered. This early return flow comprised a significant amount of vertical drainage from the unsaturated soils. The hysteresis in the unsaturated region created a strong streamward hydraulic gradient such that storage water was released more rapidly and more strongly than pre-event conditions. As the hydrograph recession proceeded, the groundwater discharge pattern returned gradually to the pre-event condition.

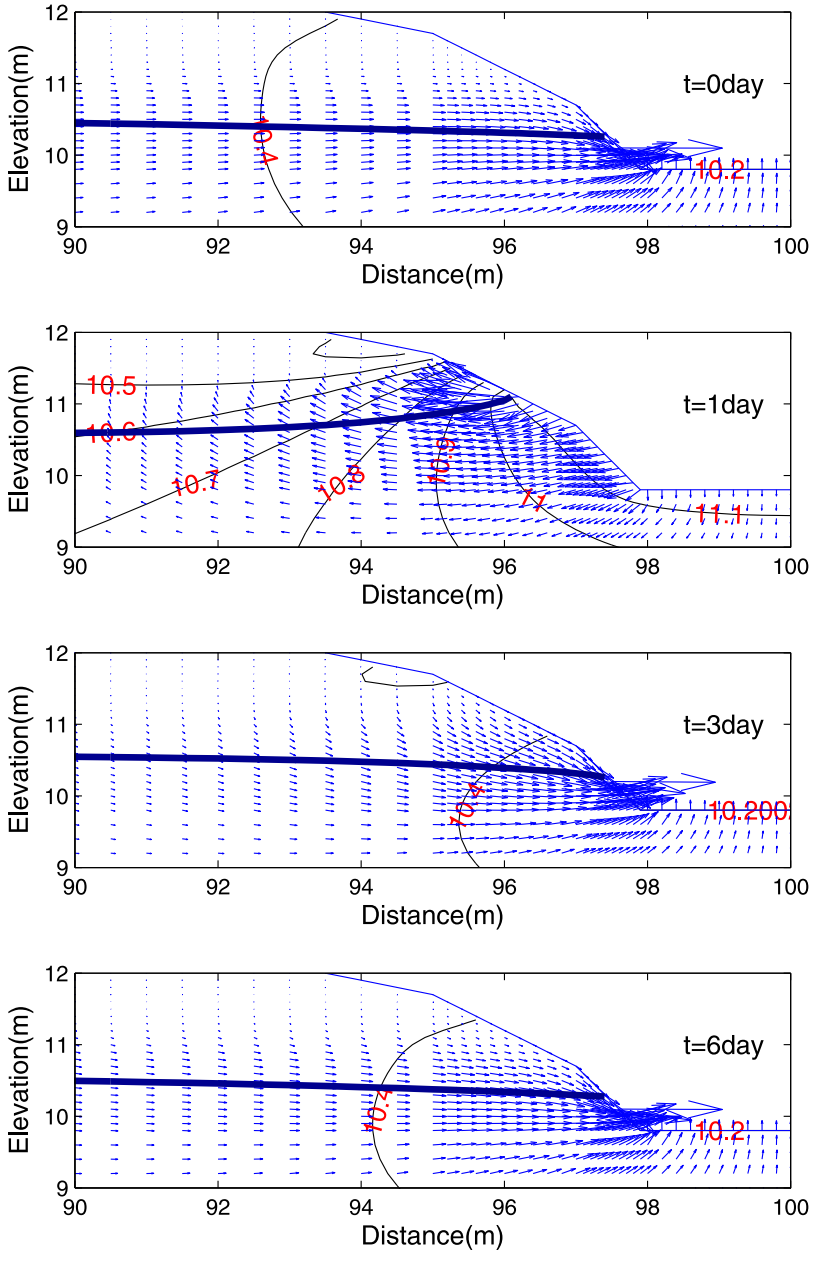

Figure 4. Average linear velocity vectors and hydraulic heads during stream stage fluctuation for the baseline simulation. The length of arrow indicates the magnitude of flow.

3.2.2. Temporal Variations of the Flow, Reaction, and NO_3^- Concentration

[29] The temporal variations of the total seepage flow occurring across the stream-riparian interface, as well as horizontal and vertical flows, are shown in the baseline simulation (Figure 5). Note the stream stage reached its peak at around $t = 0.8$ day. When stream stage rose, the groundwater seepage decreased immediately and reached negative values, thus indicating inflow of surface water. The largest infiltration rate occurred prior to the maximum stage rise, while the maximum bank storage volume $V_{max} = 5\ m^3\ m^{-1}$ occurred before the end of the stream hydrograph, when infiltrated water returned to the stream. The groundwater discharge increased gradually and reached a maximum at the end of the stream stage hydrograph, which was followed by a gradual recession. Bank storage water fully returned to the stream within about $t = 3.7$ day. The hydraulic exchange time thus, by definition, was determined as 3.7 day in this case. On the other hand, the NO_3^- mass removal rate reached the maximum near the end of return flow, which lagged behind the peak of bank storage volume by 1.5 day. The NO_3^- mass removal rate then decreased but stayed on until $t = 9$ day when NO_3^- was depleted. Figure 5e showed the flux-averaged NO_3^- concentration in seepage water. The rapid rise of NO_3^- concentration immediately after the stage rise coincided with the influx of NO_3^--rich stream water. Immediately after the streamward flow recovered and groundwater started to seep back into the stream, groundwater discharge would largely comprise mixture of groundwater and stream water that had recently entered the aquifer. Thus

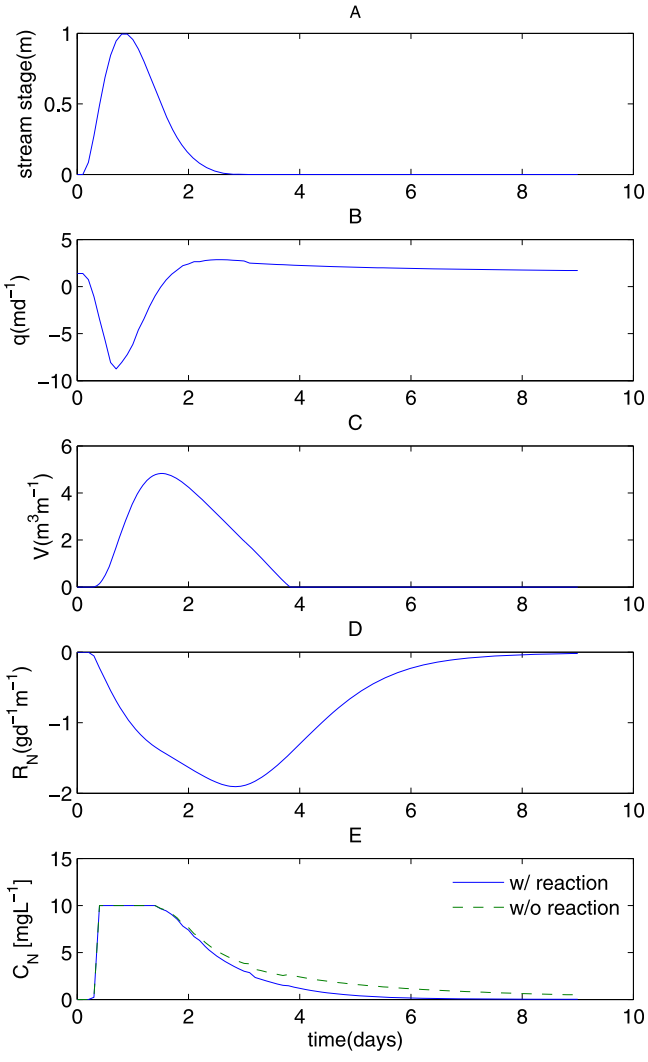

Figure 5. Temporal variation of hyporheic exchange and riparian biogeochemistry associated with stream stage fluctuation for the single-storm simulation. (a) Stream hydrograph; (b) water flux between stream and aquifer (negative fluxes indicate flows from the stream to the groundwater.); (c) volume of stream water in bank storage (m^3 m^{-1}); (d) NO_3^- mass removal rate ($g\,m^{-1}d^{-1}$); and (e) NO_3^- concentration C_N in seepage waters ($mg\,L^{-1}$) with (solid line) and without (dashed line) denitrification.

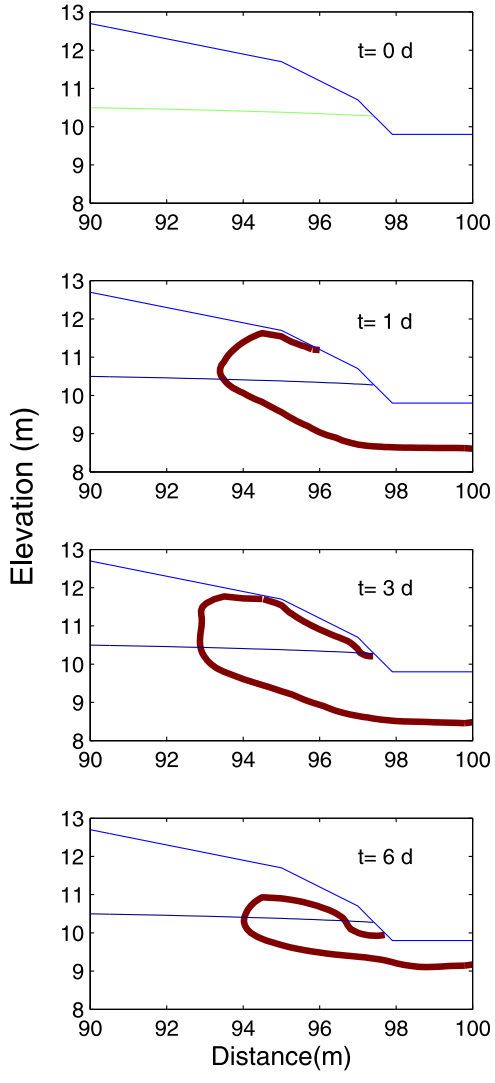

Figure 6. The temporal evolution of geochemically defined hyporheic zone that contains at least 10% stream water based on mixing ratio calculation at day 0, day 1, day 3, and day 6 for the baseline simulation.

the NO_3^- concentration in the groundwater discharge dropped when temporarily stored NO_3^--rich stream water was drained. However, NO_3^- concentration in the groundwater seepage decreased more rapidly with denitrification than that without denitrification, indicating NO_3^- removal by denitrification. In contrast to the hydraulic exchange time of 3.7 day, the NO_3^- concentration in groundwater discharge without denitrification gradually decreased and persisted until $t = 9$ day. This indicates that the chemical exchange time was much longer than the hydraulic exchange time scale.

3.2.3. Dynamics of the Hyporheic Zone

[30] Figure 6 shows the development of the riparian hyporheic zone over time, which is defined by the geochemical approach that hyporheic pore water contains at least 10% stream water in the baseline simulation. The hyporheic zone extended for about 5 m horizontally and 1.5 m vertically into the riparian aquifer at $t = 1$ day, which corresponded to the hydrograph peak and maximum stream influx rate. At $t = 3$ day, two days after the peak stage, the hyporheic zone defined by hydraulic exchange started to decrease in size because of rapid drainage of the near-stream groundwater ridge and return flow along the streambed (Figure 5c). However, the hyporheic zone defined by chemical exchange expanded further inland due to solute dispersion. At $t =$ 6 day, the hyporheic zone shrank but persisted. In contrast, the stored stream water in the streambed fully returned, as indicated by the disappearance of the hyporheic zone under the streambed (Figure 5c). The geochemically defined hyporheic zone lasted much longer than the hydraulic exchange because it included both advective and dispersive mixing between stream and groundwater.

3.2.4. DOC, NO_3^-, O_2, and Reaction Rate Distributions

[31] Modeled DOC, NO_3^-, and O_2 concentration profiles in response to stream stage fluctuations in the riparian zone are shown in the baseline simulation (Figure 7). As the stream water transported DOC from the stream into the riparian aquifer, a transient storage of DOC formed along near-stream regions (Figure 7a). This upper DOC plume persisted as long as bank storage water stayed. After the stage peak passed, the DOC plume started to reduce its size and concentration gradually when the bank storage returned water to the stream.

[32] Figure 7b shows the O_2 profiles associated with the infiltrating stream water. A rather thin layer of O_2 plume in the riparian zone was brought in by infiltrating stream water at $t = 1$ day. In contrast, NO_3^- penetrated deeper than O_2 (Figure 7c). The smaller O_2 penetration depth compared to NO_3^- and DOC can be explained by rapid O_2 consumption by the aerobic respiration of DOC. When O_2 consumption exceeded supply, an anaerobic zone was formed along the stream-riparian interface. Figure 7c also showed a trace amount of NO_3^- residue along unsaturated soils at $t = 6$ day, presumably due to the O_2 presence that inhibited denitrification.

[33] The NO_3^- reduction rate in the cross-section profile is shown in Figure 7d. The high reaction rate is evident during the bank storage event. In our simulation a distinct reaction hot spot formed around the near-stream-riparian subsurface during the stage fluctuation. The denitrification hot spot generally coincided with the O_2 depletion zone along the DOC infiltration pathway, indicating the active biogeochemical reaction was switched on by O_2 absence and simultaneous presence of NO_3^- and DOC. The reaction rate reached the peak at $t = 3$ day when O_2 was depleted while NO_3^- and DOC were present. The reaction zone shrank with vanishing DOC when bank storage water returned gradually back to the stream.

3.3. Exemplifying Simulation: Multiple Storms

[34] To study significance of the BSHM over an annual time scale, we ran the model with the stream stage fluctuation of SFNR from 29 March 2011 to 29 March 2012 (Figure 8). The mass removal rate of NO_3^-–N ranged from 0 to 10 gm^{-1} d^{-1} and showed a high temporal variation. The net removal was clearly synchronized with stage fluctuation. The larger the stage rise, the more NO_3^-–N was removed by the BSHM. This relationship was consistent with our Monte Carlo simulation results (section 3.4). The total NO_3^-–N removal per meter of stream over this one-year period was 193 g.

[35] The temporal variability in the depth-averaged DOC, O_2 concentration, denitrification rate, and NO_3^- concentration along the transect at 2, 4, and 6 m away from the stream bank, respectively, are shown in Figure 9. The smallest O_2, DOC, and NO_3^- pulse occurred at the most inland transect

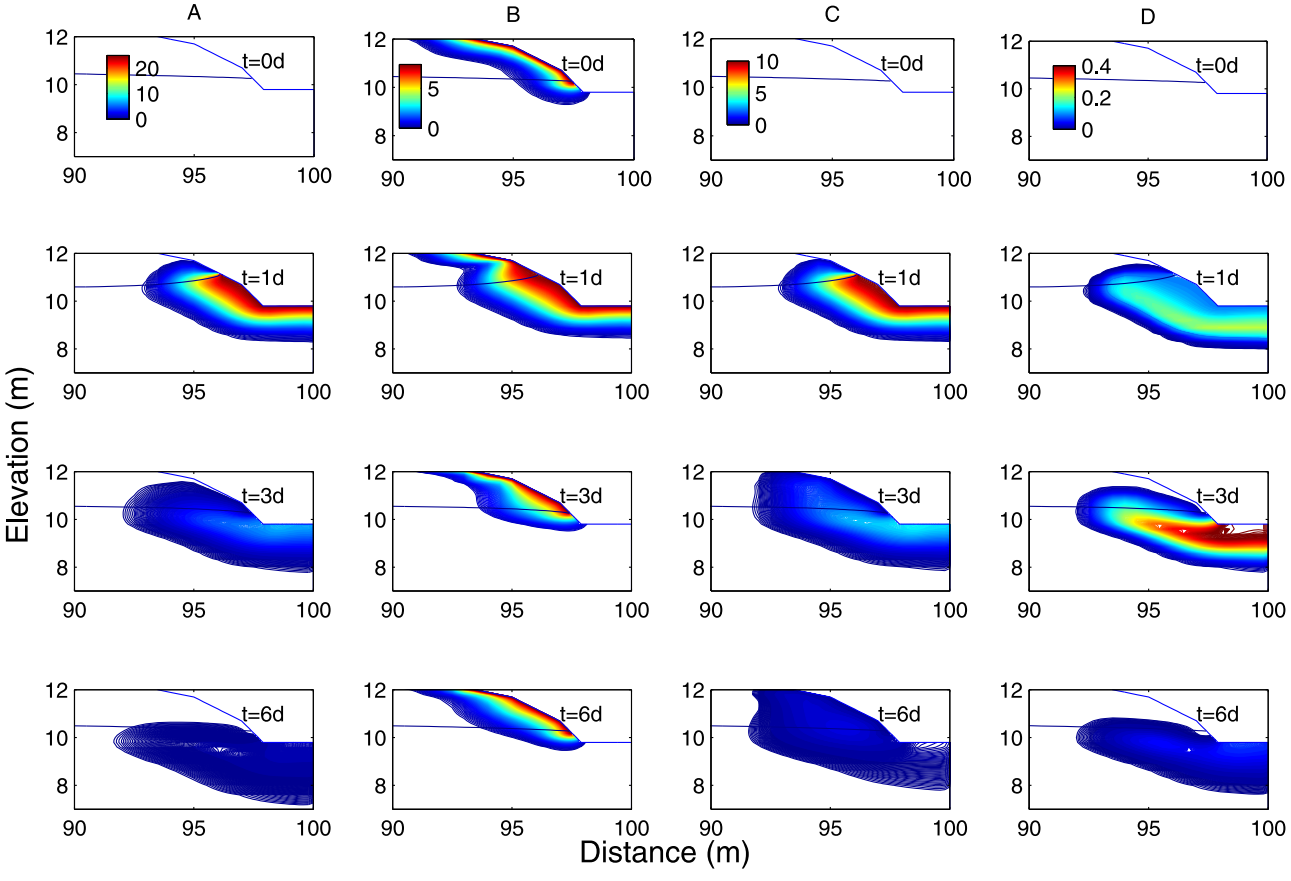

Figure 7. (a) DOC concentrations, (b) O_2 concentrations, (c) NO_3^- concentrations, and (d) reaction rates during transient stream stage fluctuation events for day 0, day 1, day 3, and day 6 after stream stage fluctuation starts for the baseline simulation.

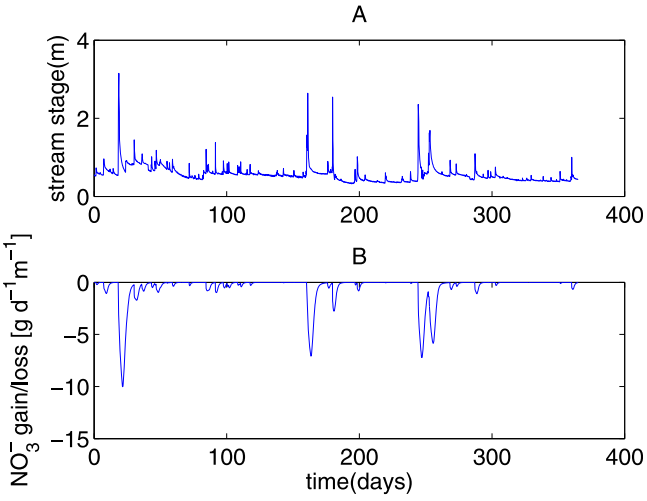

Figure 8. (a) The annual stream stage hydrograph of the SFNR and (b) the simulated temporal dynamics of NO_3^-–N removal by BSHM during 29 March 2011–29 March 2012. Note that negative values of NO_3^-–N gain/loss indicate removal.

(i.e., 6 m). As a result, also the denitrification rate were smallest there, while the high O_2, DOC, and NO_3^- pulse, and denitrification rates were associated with the streamward transects (i.e., 2 and 4 m) where the significant stream water inflow happened. Note the denitrification rate peaks occurred right after O_2 reached the minimum.

3.4. Monte Carlo Simulation Results

[36] Figure 10 shows the histogram of the maximum bank storage volume V_{max} and total mass removal rate of NO_3^- calculated as in Eq. (4) based on Monte Carlo simulations. The median value of V_{max} is 9.7 m^3 m^{-1} of stream with standard deviation (SD) of 53.2 m^3 m^{-1}. V_{max} ranged from 0 to 259 m^3 m^{-1}. The median NO_3^- mass removal rate was 2.1 g m^{-1} d^{-1} (SD = 17.2 g m^{-1} d^{-1}). The plots are characteristic of a lognormal distribution. Calculated mass removal rates ranged from 0.0 to 140.4 g m^{-1} d^{-1}. The large variability in removal rates indicated that parameter uncertainty resulted in significant sensitivity in modeling the extent of bank storage and NO_3^- removal. The large variability of NO_3^- mass removal rate was caused by the widely varying model parameters, especially hydraulic conductivity K_s that ranged from 0.1 to 100 m d^{-1}.

[37] All significant correlation ($p < 0.01$) between NO_3^- removal and the environmental variables were presented in Figure 11. The total NO_3^- removal per meter and per side of the stream was negatively correlated to the regional hydraulic gradient ($R^2 = -0.2$), and positively correlated to the hydraulic conductivity ($R^2 = 0.21$), the hydrograph amplitude ($R^2 = 0.42$), and its duration ($R^2 = 0.25$). Since all these variables control the extent of bank storage, the correlation improved significantly when we related the total NO_3^- removal and the maximum bank storage volume V_{max} ($R^2 = 0.64$) and the total NO_3^- mass brought into the riparian zone $M_{in} = V_{max} \times C$ ($R^2 = 0.65$) (Figures 12a and 12b). The strongest correlation was found ($R^2 = 0.84$) between the total mass removal and the product of M_{in}, transport time t, and reaction rate R (Figure 12c).

4. Discussion

[38] In this study we explored hydrologically driven hot moments of solute transformation using a two-dimensional flow and transport model. Our results indicate the dynamic nature of the riparian zone as a biogeochemical hot spot in response to stream stage fluctuations, hereby defined as the bank storage hot moment (BSHM). High stream stage promotes bank storage, the process in which stream water infiltrates and is temporally stored in the riparian aquifer. This flow carries a suite of reactants from the stream into the riparian subsurface where biogeochemical processes can occur. Previous research on in-stream hyporheic exchange identified stream water downwelling at the head of riffles as hot spots of biogeochemical activities [*Duff and Triska*, 2000; *Storey et al.*, 2004]. The in-stream hyporheic exchange has been identified as an important nutrient removal or regeneration processes in aquatic ecosystems [*Greenwald et al.*, 2008]. Our modeling results show that lateral expansion of the hyporheic zone at the riparian aquifer interface by bank storage can also lead to a biogeochemical hot moment that controls diffusive solute loads to surface water. To our knowledge, this is the first study to quantify the effects of stream-stage fluctuation-induced lateral hyporheic exchange on riverine contaminant transport. The current study provides an evidence to the "lung" model recently proposed by *Sawyer et al.* [2009], which describes the mixing of groundwater and surface water with distinct chemical signatures as the source of riparian biogeochemical activity. Through mathematical simulations, we are able to assess the multiple hydrological and biogeochemical factors that control the magnitude of the exchange process and the total mass removal by the biogeochemical reactions. The results show that bank storage might be critical in removal of river-borne contaminants.

4.1. Controlling Factors on the BSHM

[39] Bank storage induced two processes that regulate stream and riparian water chemistry: (1) mixing and (2) biogeochemical reactions. Previous studies indicated that groundwater-surface water mixing during bank storage can account for the variation of chemical compositions in stream water and riparian groundwater [*Fritz and Arntzen*, 2007]. This study also suggests that biogeochemical processes can alter chemical signatures of groundwater and surface water in addition to the mixing processes.

[40] As a complement to these earlier works, our study suggests that for these riparian hot moments to have a significant effect on solute fate, they must involve (1) a large mass flux into the riparian zones (i.e., a large water inflow and/or solute-rich stream water), (2) an biogeochemically active riparian sediment (i.e., a large reaction rate R), and (3) the degree of solute reaction determined by the ratio of hydraulic residence time scale to reaction time scale. The magnitude of water inflow is controlled by the spatial and temporal extent of stream-riparian interaction. Our Monte Carlo simulations show that the extent of stream-riparian exchange induced by stream stage fluctuation can be well estimated by the maximum bank storage volume (V_{max}) as an integrated index for hydrological exchange. V_{max} and total mass in M_{in} can explain 64% and 65% of the variation in the total NO_3^- removal (M), respectively. Individually, M shows much more significant correlation with V_{max} ($R^2 = 0.64$)

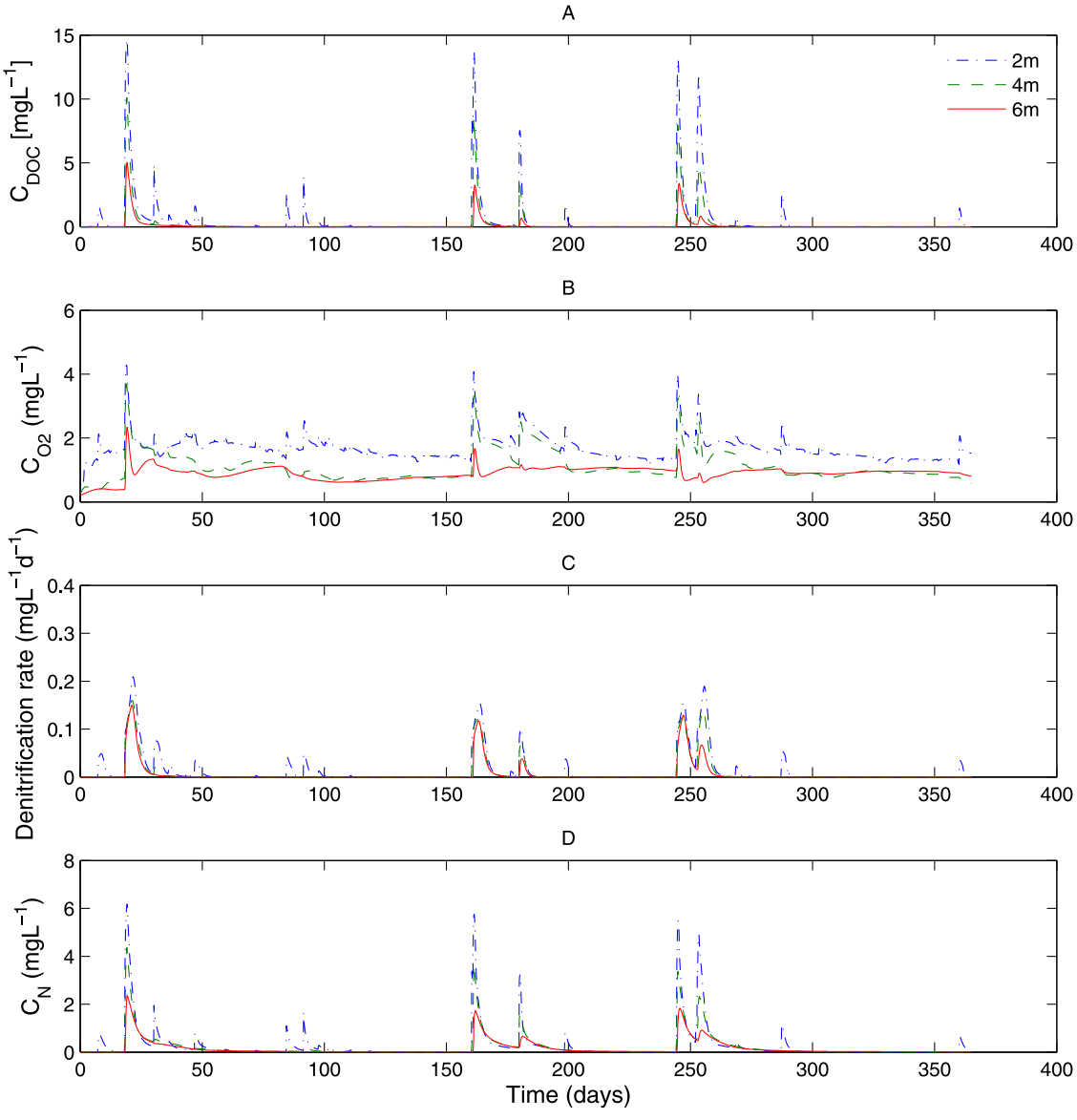

Figure 9. Depth-averaged (a) DOC concentrations C_{DOC}, (b) O_2 concentrations C_{O2}, (c) denitrification rates, and (d) NO_3^- concentrations C_N for the transects at 2, 4, and 6 m away from the stream bank for the annual simulation during 29 March 2011–29 March 2012.

than reaction rate R ($R^2 = 0.03$, data not shown). The emergence of this strong correlation between M and V_{max} despite large differences among many other characteristics of the stream (e.g., reaction rate R) suggest that the extent of hyporheic exchange rather than the biogeochemical activity dominated the variability among streams in the significance of BSHM. The large variations in hydrological controls to water exchange generated log-scale variability in hyporheic exchange. Variations in biogeochemical reaction rates due to substrate and microbial biomass concentration, as well as temperature are superimposed to the hydrologic template and will play a relatively small role in significance of BSHM. Using V_{max}, one can classify bank storage into weak, intermediate, and strong exchange. As expected the degree of biogeochemical reaction increases as the V_{max} increases. The larger the V_{max}, the longer and more extensive the contact of groundwater and surface water, and the stronger the biogeochemical hot moments. On the other hand, if this volume approaches zero and the stream-riparian exchange becomes negligible, the stream-riparian systems will remain isolated in time and space. The biogeochemical reactions that require mixing of groundwater and surface water will approach zero.

[41] The magnitude of V_{max} is determined by many parameters including aquifer transmissivity, the characteristics of the stream stage hydrograph, the stream channel geometry, the presence and absence of clogging layers around the channel, upland groundwater gradients, evapotranspiration, etc. Our correlation analysis revealed that some of these hydraulic parameters indeed influenced the total biogeochemical activity in the riparian zone because they affected V_{max}. Generally, bank storage and riparian biogeochemical hot moments were significant in a flat floodplain with coarse-grained materials and low regional

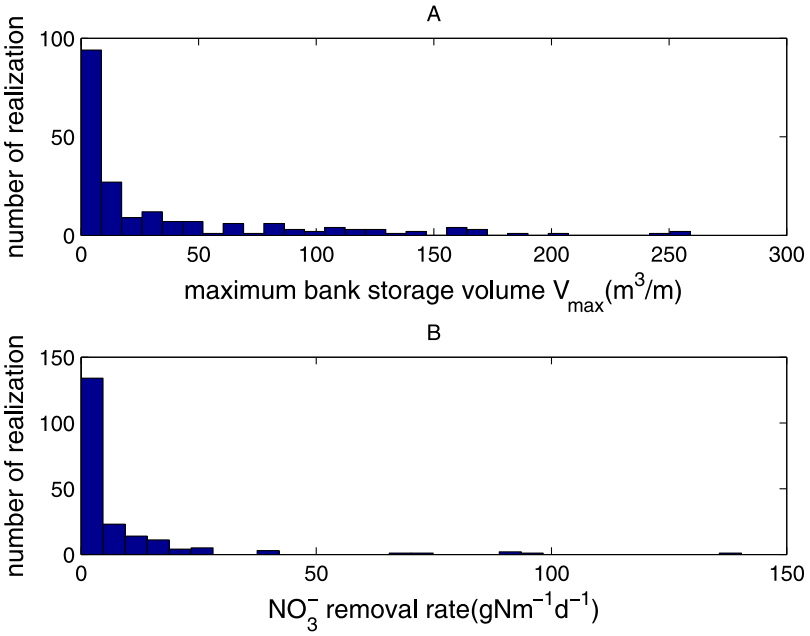

Figure 10. The histogram of (a) the maximum bank storage volume $V_{\max}$; and (b) total mass removal rate of NO_3^- based on 200 Monte Carlo simulation.

hydraulic gradient subject to high amplitude and long-lasting stream stage fluctuations, although a small magnitude of bank storage and biogeochemical hot moments indicated otherwise.

[42] For riparian hot moments to be significant, the stream-riparian zone must also be microbially active and the solute residence time has to be long enough to have a large reaction potential in addition to water inflow and mass influx. The most variability (84%) in M was explained by the product of M_{in}, transport time t, and reaction rate R, indicating that if all these four conditions are met, riparian hot moments are much more likely to affect reactive solute transport and mass balance significantly. The relationship can be derived using a mathematical framework. We suggest a dimensionless significance index I_s, the efficiency of solute removal in bank storage, for the cumulative effect of riparian hot moments be defined as

$$I_S = \frac{\int_0^t R}{\int_0^t qC} = \frac{M}{V_{\max} C} = f(k \times t), \tag{10}$$

where R is the biogeochemical reaction rate ($\mathrm{M\,T^{-1}}$), q is the stream water flux into the riparian zone ($\mathrm{L^3\ T^{-1}}$), C is the solute concentration of stream water ($\mathrm{M\,L^{-3}}$), $V_{\max}$ is the maximum bank storage volume ($\mathrm{L^3}$), k is the first order reaction rate constant ($\mathrm{T^{-1}}$), t is the solute contact time with the riparian zones, and M is the total mass removal (M). $V_{\max} \times C$ (M) is the time cumulative mass transported into the riparian zones (M). Values of I_s (i.e., Damkohler number), defined as the ratio of characteristic transport time scale to characteristic reaction time scale, represent the effectiveness of riparian hot moments on stream-derived contaminant removal. All the solute exchanged is completely consumed in the riparian zone when I_s equals one. In this case, the nutrient retention is limited by the solute influx but not the solute residence time. While there is no contaminant removal when I_s approaches zero, which means the removal is limited by the residence time. Finally, the removal is limited by both the solute influx and the residence time within the riparian zones when I_s lies between 0 and 1. With information on biogeochemical activity and estimates of the extent of bank storage, one can rank streams into broad classes of effectiveness of BSHM based on equation (10). For instance, if an extensive bank storage event that passes solute-rich stream waters through biogeochemically active sediments, the BSHM will be substantial. The opposite case is represented by small exchange volumes with solute-poor stream waters and inactive sediments. A similar significance index that integrates hydrological and biogeochemical factors was developed by *Harvey and Fuller* [1998] to quantify the significance of hyporheic uptake of reactive solutes based on the balance between chemical reaction rates, hyporheic residence time, and turnover of streamflow through hyporheic flow paths. *Gu et al.* [2007] also suggested that hydrological time scales must be similar or larger than biogeochemical time scales to allow significant biogeochemical processes to occur in the stream sediments. This scheme would allow us to uncover generalities across varying stream systems.

4.2. Other Important Riparian Biogeochemical Processes

[43] Note that other major N cycling processes such as ammonification and nitrification were not taken into account in this study. Whether or not riparian zones serve as a NO_3^- source or sink during biogeochemical hot moments is controlled by the overall nitrogen reaction networks. There are probably coexisting aerobic and anaerobic zones in the hyporheic sediments. Rapid depletion of oxygen in the infiltrating stream water through aerobic respiration is not uncommon in hyporheic sediments. This would lead to a strong oxic-anoxic

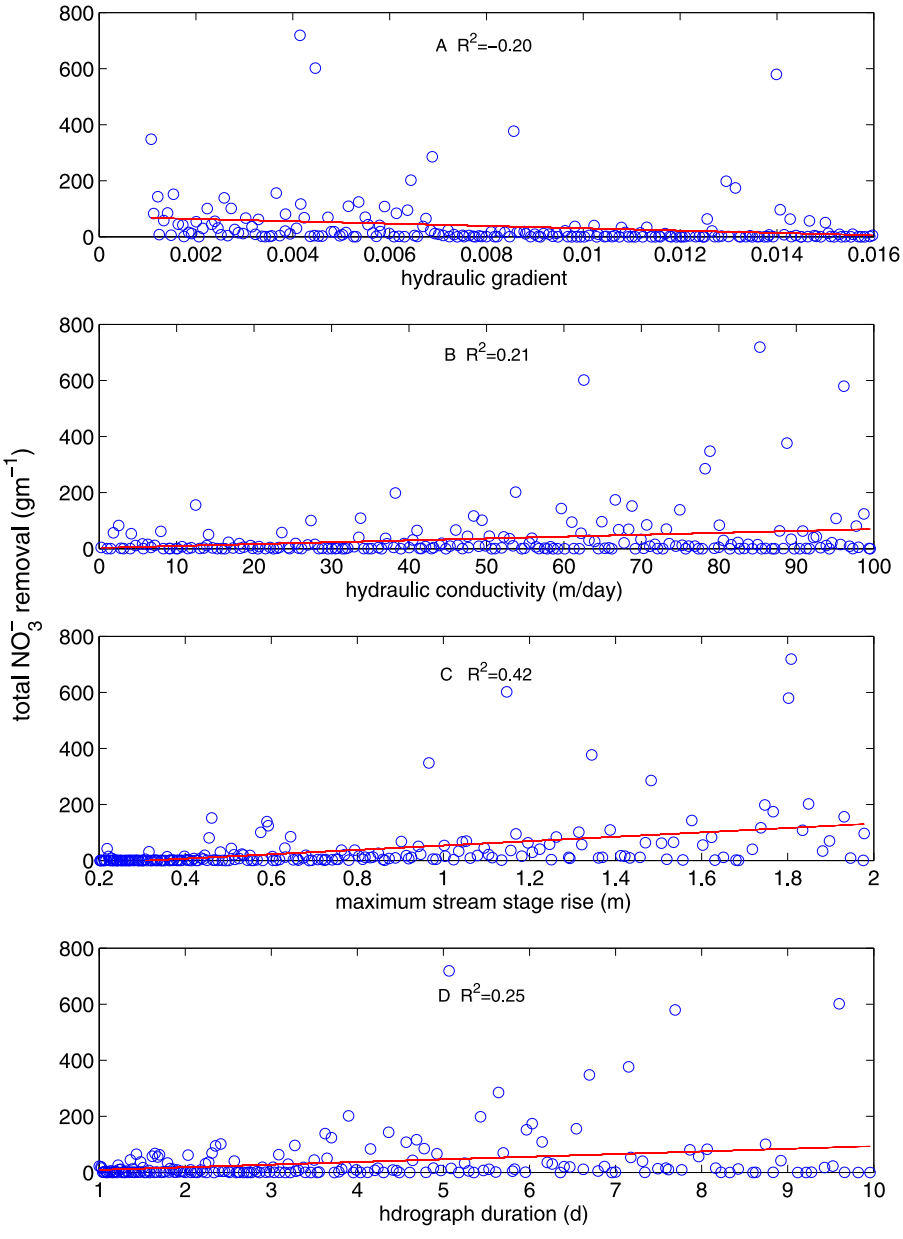

Figure 11. Linear regression results between the total NO_3^- removal ($g\,m^{-1}$) and (a) hydraulic gradient; (b) hydraulic conductivity; (c) maximum stream stage rise; and (d) hydrograph duration based on 200 Monte Carlo simulation results.

boundary where groundwater, stream water, and pore water mix or where oxygen depletion occurs due to high rates of aerobic metabolism. This interface provides an opportunity for rapid nitrogen cycling and efficient nitrogen removal or regeneration from the system. The net NO_3^- production and consumption depends on the balance between nitrification and denitrification [*Maggi et al.*, 2008]. *Zarnetske et al.* [2011] suggest that the hyporheic zone as nitrogen sink or source depends on residence time. The net NO_3^- production by nitrification was greatest during short residence time while NO_3^- removal by denitrification was greatest at long residence time. This is because organic matter in the hyporheic zone is mineralized to ammonium, which can be transformed into NO_3^- by nitrification in aerobic zones. If the aerobic zone is close to an anaerobic zone, NO_3^- can be reduced and exported from the system as a gas to the atmosphere through the denitrification process [*Duff and Triska*, 2000]. It is possible that in streams with a strong groundwater discharge subject to a small stream stage fluctuation, hyporheic exchange would be relatively rapid and limited in extent. As a result, anaerobic sites in the hyporheic zone would be less common and nitrification would be dominant, causing riparian zones to be a NO_3^- source. In low groundwater gradient streams in response to large stream stage fluctuation, the hyporheic exchange might be slow and extensive. Consequently, denitrification might be more important under anaerobic conditions, which makes riparian zones a net NO_3^- sink. Further study is needed to study this coupled nitrification-denitrification

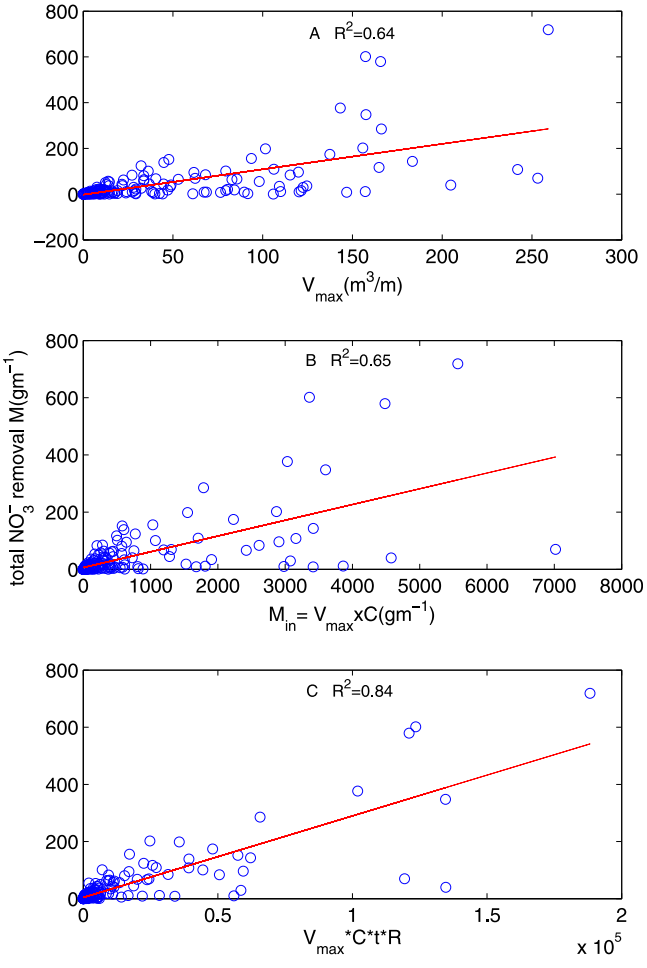

Figure 12. Relationship between the total mass removal M and (a) the maximum bank storage volume $V_{\max}$; (b) the total solute mass brought in by infiltrating stream water $M_{\text{in}} = V_{\max} \times C$, where C is the NO_3^- concentration in the stream, and (c) the product of M_{in}, transport time t, and reaction rate R. (Note that we used the zero-order reaction rate constant R instead of a first order rate constant k in equation (10).) Circles indicate Monte Carlo simulation results.

process as the biogeochemical hot moment during stream stage fluctuation.

[44] It is worth mentioning that although this study took NO_3^- reduction by denitrification as an illustration of biogeochemical process in the riparian zone, the conclusion drawn by this study is generic and should also be applicable to other biogeochemical processes such as sulfate reduction, iron reduction, and aerobic biodegradation of organic pollutants, etc. The stream water chemicals other than DOC that might trigger biogeochemical hot spots at the riparian zone include temperature, oxygen, and other macro and micro nutrients. Furthermore, the BSHM might play a role in buffering terrestrial pollutants in addition to stream water chemistry, as the riparian buffer was widely used to protect surface water quality. For example, land-derived NO_3^- was subject to the same consumption process as stream-derived NO_3^- in our study. Thus the potential of riparian buffers to remove groundwater pollutants during the BSHM is equally important. We present a sample analysis on the significance of BSHM on in-stream NO_3^- transport in the following section.

4.3. Significance of the Hot Moment on Nutrient Balance

[45] To evaluate the importance of BSHM with respect to N export from watersheds, we compare BSHM with in-stream N uptake, an intensively studied N retention mechanism in streams [e.g., *Peterson et al.*, 2001]. We compiled several major storage metrics (Q_L, α, T_s, and A_s/A) and NO_3^- uptake metrics (U and V_f) for transient storage from the literatures (Table 2). We then calculated the same metrics for bank storage based on the data generated from the Monte Carlo simulation. The lateral inflow per length of stream Q_L in transient storage and bank storage were 5.9 and 10.4 $m^3\,d^{-1}\,m^{-1}$, respectively, which indicated comparable water flux through storage zone in bank storage compared to transient storage. The storage exchange coefficient α, the lateral inflow normalized by the stream cross section area ($=Q_L/A$), of bank storage were lower than that of transient storage. On the other hand, residence time in storage zone and normalized storage area were about 29-fold and 4-fold higher in bank storage than in transient storage. Comparisons of NO_3^- uptake between bank storage and transient storage was accomplished by using areal uptake rate (U, NO_3^- mass removal per unit area of streambed per unit time) and uptake velocity (V_f, vertical velocity of NO_3^- through the water column toward the streambed). These metrics of NO_3^- uptake are preferred metric over uptake length (S_w) because they are independent of stream discharge [*Ensign and Doyle*, 2006]. U was about 22-fold greater in bank storage than in transient storage, suggesting strong NO_3^- uptake potential in bank storage. Since U is a

Table 2. Comparison of Storage and NO_3^- Uptake Metrics Between In-Stream Transient Storage and Bank Storage Processes[a]

Metric	Name	Symbol	Transient Storage Median (SD)	Bank Storage Median (SD)
Transient Storage Metrics	Lateral Inflow Per Unit Length of Stream	Q_L ($m^3\,m^{-1}\,d^{-1}$)	5.9 (7.6)	10.4 (22)
	Storage Exchange Coefficient[b]	α (s^{-1})	3.5×10^{-4} (2.1×10^{-4})	7.5×10^{-5} (1.6×10^{-4})
	Residence Time in Storage Zone[b]	T_s (min)	286.7 (321)	2.5×10^{3} (5.1×10^{3})
	Normalized Area of Storage Zone[b]	A_s/A	1.4 (4.6)	6 (33.3)
Nitrate Uptake Metrics	Areal Uptake Rate[c]	U ($\mu g m^{-2}\,min^{-1}$)	16.7	362 (3.0×10^{3})
	Uptake Velocity[c]	V_f ($m\,min^{-1}$)	6×10^{-5}	2.7×10^{-5} (2.4×10^{-4})

[a]The detailed definition and derivation of these metrics can be found in *Stream Solute Workshop* [1990].
[b][*Lautz and Siegel*, 2007].
[c][*Mulholland et al.*, 2008]

function of NO_3^- concentration, we also compared V_f, normalized U by NO_3^- concentration (U/C). V_f in bank storage was lower than that in transient storage. One can see that bank storage, if it occurs, can induce a similar magnitude of hydraulic exchange and solute removal to in-stream nutrient spiraling processes caused by transient storage. Since transient storage becomes less efficient at removing nutrients at high flow conditions [*Hall et al.*, 2002], bank storage and transient storage might complement each other in the way that transient storage is dominant during base flow while bank storage takes over during high flow in regard to nutrient retention.

[46] Despite its NO_3^- retention capacity, the significance of the riparian hot moment might be limited by the transient nature of stream-riparian interactions, which only occurs during episodic hydrological events in contrast to steady state in-stream hyporheic exchange, e.g., channel bed form induced [*Cardenas and Wilson*, 2007], under base flow conditions. To investigate whether BSHM is significant with respect to long-term nutrient uptake, we conducted a simulation of stream-riparian interaction based on the observed hydrograph at our site from 29 March 2011 to 29 March 2012 (Figure 9). Our results showed a total NO_3^- removal of 193 $g\,m^{-1}$ of stream. In comparison, the annual mean in-stream NO_3^- mass removal due to nutrient spiraling is 35.11 $g\,m^{-1}$, assuming a 4 m wide headwater stream and a median in-stream NO_3^- uptake rate of 16.7 $\mu g\ m^{-2}\ min^{-1}$. One can see the BSHM is a potential significant nutrient retention mechanism at long time scales.

[47] In addition, the time span of stream-riparian interaction can be prolonged depending on the water table dynamics. The stream can become a dominant control on riparian water table gradients, particularly in flat floodplains [*Vidon and Hill*, 2004b]. During dry periods, water table gradients could reverse from streamward to landward [*Burt et al.*, 2002; *Duval and Hill*, 2006]. During this period, stream-origin groundwater extends all the way to the field edge, effectively extending the hyporheic zone throughout the riparian area [*Duval and Hill*, 2007]. Denitrification has been identified to be responsible for some of the observed NO_3^- losses as stream water moved inland by tracking NO_3^- injections with a bromide tracer. These studies demonstrate that base flow bank infiltration can be a dominant control on riparian hydrology and biogeochemistry.

[48] Finally, dam operations and diel snow melt also create short, but frequent, flow dynamics, inducing large amounts of surface water in and out the riparian aquifer. The near-stream-riparian aquifer thus serves as a natural biogeochemical reactor that alters the chemical signatures of surface water and groundwater discharge, either improving or degrading their quality depending on what reactions occur. In general, the rivers experiencing pronounced and prolonged water table fluctuations are likely subject to significant biogeochemical alteration. The impacts on chemical transport at watershed scales can be significant because stage fluctuation-induced hyporheic exchange occurs relatively briefly yet over much larger spatial scales than the in-stream hyporheic exchange.

5. Conclusion

[49] In this study we have focused on the hyporheic exchanges in riparian zones induced by stream stage fluctuations, referred to as bank storage. We have investigated (1) how bank storage can influence riverine transport of contaminants such as nitrate, (2) how this effect changed with hydrobiogeochemical factors, and (3) how significant the effect is with respect to riverine nitrate transport. The biogeochemical processes during bank storage were analyzed using a two-dimensional, variably saturated flow and multispecies reactive transport model. The model captured field-collected water table and temperature dynamics reasonably well. Using an exemplifying numerical simulation, we have shown that high biogeochemical activities occurred at the near-stream riparian zone, a process defined as bank storage hot moment (BSHM). The stochastic models of varying hydraulic and biogechemical conditions showed that stream fluctuations can lead to maximum bank storage volume ranging from 0 to 259 $m^3\,m^{-1}$ of river channel. Taking denitrification as the example, a BSHM can lead to a median removal of 2.1 g NO_3^- per meter of river channel. The sensitivity of BSHM and related nutrient dynamics to biogeochemical and hydrological factors were analyzed using Monte Carlo simulations. This result suggested that a BSHM may be a significant process contributing to the nutrient budget at the ecosystem level. The primary controls on BSHM are the residence time, bank storage volume, and denitrification rate. Consequently, a significance index representing the coupled hydrobiogeochemical controls on riparian hot spots was developed to help predicting when BSHM can become important in a particular stream. The generalization that focuses on a single stream stage fluctuation in this study will help to categorize watersheds with regard to their significance of biogeochemical hot moments per individual hydrological disturbance.

[50] **Acknowledgments.** We would like to thank the University Research Council at Appalachian State University for funding this project partially. We would like to thank Jeff Colby for help with fieldwork and Mei Yi for his help with the numerical simulations. Discussion with G. Hornberger helped improve this manuscript. The authors also thank the Associated Editor and two anonymous reviewers for their helpful comments that have helped to improve the quality of the manuscript.

References

Allan, C. J., P. Vidon, and R. Lowrance (2008), Frontiers in riparian zone research in the 21st century, *Hydrol. Processes*, *22*(16), 3221–3222, doi:10.1002/Hyp.7086.

Anderson, W. P., R. E. Storniolo, and J. S. Rice (2011), Bank thermal storage as a sink of temperature surges in urbanized streams, *J. Hydrol.*, *409*(1–2), 525–537, doi:10.1016/j.jhydrol.2011.08.059.

Bailey, B. L., S. T. Marshall, and W. P. Anderson (2010), Integrating ground penetrating radar, electrical resistivity, seismic refraction, and borehole data to image an alluvial aquifer in three dimensions, Abstract H13D-1000 presented at 2010 AGU Fall Meeting, AGU, San Francisco, Calif., 13–17 Dec.

Baillie, M. N., J. F. Hogan, B. Ekwurzel, A. K. Wahi, and C. J. Eastoe (2007), Quantifying water sources to a semiarid riparian ecosystem, San Pedro River, Arizona, *J. Geophys. Res. Biogeosci.*, *112*(G3), G03s02.

Baker, M. A., C. N. Dahm, and H. M. Valett (1999), Acetate retention and metabolism in the hyporheic zone of a mountain stream, *Limnol. Oceanogr.*, *44*(6), 1530–1539.

Baker, M. A., H. M. Valett, and C. N. Dahm (2000), Organic carbon supply and metabolism in a shallow groundwater ecosystem, *Ecology*, *81*(11), 3133–3148.

Bates, P. D., M. D. Stewart, A. Desitter, M. G. Anderson, J. P. Renaud, and J. A. Smith (2000), Numerical simulation of floodplain hydrology, *Water Resour. Res.*, *36*(9), 2517–2529.

Boano, F., R. Revelli, and L. Ridolfi (2008), Reduction of the hyporheic zone volume due to the stream-aquifer interaction, *Geophys. Res. Lett.*, *35*(9), L09401, doi:10.1029/2008GL033554.

Boutt, D. F., and B. J. Fleming (2009), Implications of anthropogenic river stage fluctuations on mass transport in a valley fill aquifer, *Water Resour. Res.*, *45*, W04427, doi:10.1029/2007WR006526.

Boyer, E. W., G. M. Hornberger, K. E. Bencala, and D. M. Mcknight (1997), Response characteristics of DOC flushing in an alpine catchment, *Hydrol. Processes*, *11*(12), 1635–1647.

Brooks, R. H., and A. T. Corey (1966), Properties of porous media affecting fluid flow, *J. Irrig. Drain. Div.*, *92*(IR2), 61–88.

Burt, T. P., G. Pinay, F. E. Matheson, N. E. Haycock, A. Butturini, J. C. Clement, and V. Maitre (2002), Water table fluctuations in the riparian zone: Comparative results from a pan-European experiment, *J. Hydrol.*, *265*(1–4), 129–148.

Cardenas, M. B., and J. L. Wilson (2006), The influence of ambient groundwater discharge on exchange zones induced by current-bedform interactions, *J. Hydrol.*, *331*(1–2), 103–109, doi:10.1016/j.jhydrol.2006.05.012.

Cardenas, M. B., and J. L. Wilson (2007), Dunes, turbulent eddies, and interfacial exchange with permeable sediments, *Water Resour. Res.*, *43*(8), W08412, doi:10.1029/2006WR005787.

Cey, E. E., D. L. Rudolph, R. Aravena, and G. Parkin (1999), Role of the riparian zone in controlling the distribution and fate of agricultural nitrogen near a small stream in southern Ontario, *J. Contam. Hydrol.*, *37*(1–2), 45–67.

Chanat, J. G., and G. M. Hornberger (2003), Modeling catchment-scale mixing in the near-stream zone—Implications for chemical and isotopic hydrograph separation, *Geophys. Res. Lett.*, *30*(2), 1091, doi:10.1029/2002GL016265.

Chen, X., and X. H. Chen (2003), Stream water infiltration, bank storage, and storage zone changes due to stream-stage fluctuations, *J. Hydrol.*, *280*(1–4), 246–264, doi:10.1016/S0022-1694(03)00232-4.

Chen, Y. M., L. M. Abriola, P. J. J. Alvarez, P. J. Anid, and T. M. Vogel (1992), Modeling transport and biodegradation of benzene and toluene in sandy aquifer material—Comparisons with experimental measurements, *Water Resour. Res.*, *28*(7), 1833–1847.

Cirmo, C. P., and J. J. McDonnell (1997), Linking the hydrologic and biogeochemical controls of nitrogen transport in near-stream zones of temperate-forested catchments: A review, *J. Hydrol.*, *199*(1–2), 88–120.

Cooley, R. L. (1983), Some new procedures for numerical-solution of variably saturated flow problems, *Water Resour. Res.*, *19*(5), 1271–1285.

Cooper, H., Jr., and M. I. Rorabaugh (1963), Ground-water movements and bank storage due to flood stages in surface stream, *U.S. Geol. Surv. Water Sup. Pap.*, *1536-J*, 343–366.

Dahm, C. N., N. B. Grimm, P. Marmonier, H. M. Valett, and P. Vervier (1998), Nutrient dynamics at the interface between surface waters and groundwaters, *Freshwater Biol.*, *40*(3), 427–451.

Devito, K. J., D. Fitzgerald, A. R. Hill, and R. Aravena (2000), Nitrate dynamics in relation to lithology and hydrologic flow path in a river riparian zone, *J. Environ. Qual.*, *29*(4), 1075–1084.

Doble, R., P. Brunner, J. McCallum, and P. G. Cook (2012), An analysis of river bank slope and unsaturated flow effects on bank storage [Research Support, Non-U.S. Gov't]. *Ground Water*, *50*(1), 77–86. doi:10.1111/j.1745-6584.2011.00821.x.

Doussan, C., G. Poitevin, E. Ledoux, and M. Detay (1997), River bank filtration: Modelling of the changes in water chemistry with emphasis on nitrogen species, *J. Contam. Hydrol.*, *25*(1–2), 129–156.

Duff, J. H., and F. J. Triska (2000). *Nitrogen Biogeochemistry and Surface-Subsurface Exchange in Streams*, Academic, London.

Duval, T. P., and A. R. Hill (2006), Influence of stream bank seepage during low-flow conditions on riparian zone hydrology, *Water Resour. Res.*, *42*(10), W10425, doi:10.1029/2006WR004861.

Duval, T. P., and A. R. Hill (2007), Influence of base flow stream bank seepage on riparian zone nitrogen biogeochemistry, *Biogeochemistry*, *85*(2), 185–199, doi:10.1007/s10533-007-9128-9.

Ensign, S. H., and M. W. Doyle (2006), Nutrient spiraling in streams and river networks, *J. Geophys. Res. Biogeosci.*, *111*(G4), G04009.

Fetter, C. W. (2001), *Applied Hydrogeology*, 4th ed., Prentice Hall, Englewood Cliffs, NJ.

Findlay, S. (1995), Importance of surface-subsurface exchange in stream ecosystems—The hyporheic zone, *Limnol. Oceanogr.*, *40*(1), 159–164.

Fritz, B. G., and E. V. Arntzen (2007), Effect of rapidly changing river stage on uranium flux through the hyporheic zone, *Ground Water*, *45*(6), 753–760, doi:10.1111/j.1745-6584.2007.00365.x.

Gelhar, L. W., C. Welty, and K. R. Rehfeldt (1992), A critical-review of data on field-scale dispersion in aquifers, *Water Resour. Res.*, *28*(7), 1955–1974.

Gerecht, K. E., M. B. Cardenas, A. J. Guswa, A. H. Sawyer, J. D. Nowinski, and T. E. Swanson (2011), Dynamics of hyporheic flow and heat transport across a bed-to-bank continuum in a large regulated river, *Water Resour. Res.*, *47*, W03524, doi:10.1029/2010WR009794.

Gold, A. J., P. M. Groffman, K. Addy, D. Q. Kellogg, M. Stolt, and A. E. Rosenblatt (2001), Landscape attributes as controls on ground water nitrate removal capacity of riparian zones, *J. Am. Water Resour. Assoc.*, *37*(6), 1457–1464.

Greenwald, M. J., W. B. Bowden, M. N. Gooseff, J. P. Zarnetske, J. P. McNamara, J. H. Bradford, and T. R. Brosten (2008), Hyporheic exchange and water chemistry of two arctic tundra streams of contrasting geomorphology, *J. Geophys. Res. Biogeosci.*, *113*(G2), G02029.

Gu, C. H., G. M. Hornberger, A. L. Mills, J. S. Herman, and S. A. Flewelling (2007), Nitrate reduction in streambed sediments: Effects of flow and biogeochemical kinetics, *Water Resour. Res.*, *43*(12). W12413, doi:10.1029/2007WR006027.

Gu, C. H., G. M. Hornberger, J. S. Herman, and A. L. Mills (2008a), Effect of freshets on the flux of groundwater nitrate through streambed sediments, *Water Resour. Res.*, *44*(5), W05415, doi:10.1029/2007WR006488.

Gu, C. H., G. M. Hornberger, J. S. Herman, and A. L. Mills (2008b), Influence of stream-groundwater interactions in the streambed sediments on NO_3^- flux to a low-relief coastal stream, *Water Resour. Res.*, *44*(11), W11432, doi:10.1029/2007WR006739.

Hall, R. O., E. S. Bernhardt, and G. E. Likens (2002), Relating nutrient uptake with transient storage in forested mountain streams, *Limnol. Oceanogr.*, *47*(1), 255–265.

Hanson, G. C., P. M. Groffman, and A. J. Gold (1994), Denitrification in riparian wetlands receiving high and low groundwater nitrate inputs, *J. Environ. Qual.*, *23*(5), 917–922.

Harvey, J. W., and C. C. Fuller (1998), Effect of enhanced manganese oxidation in the hyporheic zone on basin-scale geochemical mass balance, *Water Resour. Res.*, *34*(4), 623–636.

Hedin, L. O., J. C. von Fischer, N. E. Ostrom, B. P. Kennedy, M. G. Brown, and G. P. Robertson (1998), Thermodynamic constraints on nitrogen transformations and other biogeochemical processes at soil-stream interfaces, *Ecology*, *79*(2), 684–703.

Hill, A. R. (1996), Nitrate removal in stream riparian zones, *J. Environ. Qual.*, *25*(4), 743–755.

Hill, A. R., K. J. Devito, S. Campagnolo, and K. Sanmugadas (2000), Subsurface denitrification in a forest riparian zone: Interactions between hydrology and supplies of nitrate and organic carbon, *Biogeochemistry*, *51*(2), 193–223.

Hornberger, G. M., K. E. Bencala, and D. M. Mcknight (1994), Hydrological controls on dissolved organic-carbon during snowmelt in the Snake River near Montezuma, Colorado, *Biogeochemistry*, *25*(3), 147–165.

Iman, R. L., and J. C. Helton (1988), An investigation of uncertainty and sensitivity analysis techniques for computer-models, *Risk Anal.*, *8*(1), 71–90.

Inamdar, S. P., and M. J. Mitchell (2006), Hydrologic and topographic controls on storm-event exports of dissolved organic carbon (DOC) and nitrate across catchment scales, *Water Resour. Res.*, *42*(3), W03421, doi:10.1029/2005WR004212.

Kasahara, T., and A. R. Hill (2006), Effects of riffle-step restoration on hyporheic zone chemistry in N-rich lowland streams, *Can. J. Fish. Aquatic Sci.*, *63*(1), 120–133, doi:10.1139/F05-199.

Kaushal, S. S., P. M. Groffman, P. M. Mayer, E. Striz, and A. J. Gold (2008), Effects of stream restoration on denitrification in an urbanizing watershed [Research Support, U.S. Gov't, Non-P.H.S.], *Ecol. Appl*, *18*(3), 789–804.

Kindred, J. S., and M. A. Celia (1989), Contaminant transport and biodegradation. 2. Conceptual-model and test simulations, *Water Resour. Res.*, *25*(6), 1149–1159.

Lautz, L. K., and D. I. Siegel (2007), The effect of transient storage on nitrate uptake lengths in streams: An inter-site comparison, *Hydrol. Processes*, *21*(26), 3533–3548, doi:10.1002/Hyp.6569.

Lee, M. S., K. K. Lee, Y. J. Hyun, T. P. Clement, and D. Hamilton (2006), Nitrogen transformation and transport modeling in groundwater aquifers, *Ecol. Model.*, *192*(1–2), 143–159, doi:10.1016/j.ecolmodel.2005.07.013.

Loheide, S. P., and J. D. Lundquist (2009), Snowmelt-induced diel fluxes through the hyporheic zone, *Water Resour. Res.*, *45*, W07404, doi:10.1029/2008WR007329.

MacQuarrie, K. T., E. A. Sudicky, and W. D. Robertson (2001), Numerical simulation of a fine-grained denitrification layer for removing septic system nitrate from shallow groundwater [Research Support, Non-U.S. Gov't], *J. Contam. Hydrol.*, *52*(1–4), 29–55.

Maggi, F., C. Gu, W. J. Riley, G. M. Hornberger, R. T. Venterea, T. Xu, and C. M. Oldenburg (2008), A mechanistic treatment of the dominant

soil nitrogen cycling processes: Model development, testing, and application, *J. Geophys. Res. Biogeosci.*, *113*(G2), G02016.

McCallum, J. L., P. G. Cook, P. Brunner, and D. Berhane (2010), Solute dynamics during bank storage flows and implications for chemical base flow separation, *Water Resour. Res.*, *46*, W07541, doi:10.1029/2009WR008539.

McClain, M. E., E. W. Boyer, C. L. Dent, S. E. Gergel, N. B. Grimm, P. M. Groffman, and G. Pinay (2003). Biogeochemical hot spots and hot moments at the interface of terrestrial and aquatic ecosystems, *Ecosystems*, *6*(4), 301–312, doi:10.1007/s10021-003-0161-9.

McGlynn, B. L., and J. J. McDonnell (2003), Quantifying the relative contributions of riparian and hillslope zones to catchment runoff, *Water Resour. Res.*, *39*(11), 1310, doi:10.1029/2003WR002091.

Mulholland, P. J., A. M. Helton, G. C. Poole, R. O. Hall, S. K. Hamilton, B. J. Peterson, and S. M. Thomas (2008), Stream denitrification across biomes and its response to anthropogenic nitrate loading [Research Support, U.S. Gov't, Non-P.H.S.], *Nature*, *452*(7184), 202–205, doi:10.1038/nature06686.

Neuman, S. P. (1990), Universal scaling of hydraulic conductivities and dispersivities in geologic media, *Water Resour. Res.*, *26*(8), 1749–1758.

Peterson, B. J., et al. (2001), Control of nitrogen export from watersheds by headwater streams, *Science*, *292*, 86–90.

Pinay, G., L. Roques, and A. Fabre (1993), Spatial and temporal patterns of denitrification in a riparian forest, *J. Appl. Ecol.*, *30*(4), 581–591.

Rassam, D. W., C. S. Fellows, R. De Hayr, H. Hunter, and P. Bloesch (2006), The hydrology of riparian buffer zones; two case studies in an ephemeral and a perennial stream, *J. Hydrol.*, *325*(1–4), 308–324, doi:10.1016/j.jhydrol.2005.10.023.

Sawyer, A. H., M. B. Cardenas, A. Bomar, and M. Mackey (2009), Impact of dam operations on hyporheic exchange in the riparian zone of a regulated river, *Hydrol. Processes*, *23*(15), 2129–2137, doi:10.1002/Hyp.7324.

Schlesinger, W. H. (1997), *Biogeochemistry: An analysis of Global Change*, 2nd ed., Academic, New York.

Squillace, P. J. (1996), Observed and simulated movement of bank-storage water, *Ground Water*, *34*(1), 121–134.

Storey, R. G., D. D. Williams, and R. R. Fulthorpe (2004), Nitrogen processing in the hyporheic zone of a pastoral stream, *Biogeochemistry*, *69*(3), 285–313.

Stream Solute Workshop (1990), Concepts and methods for assessing solute dynamics in stream ecosystems, *J. North Am. Benthol. Soc.*, *9*(2), 95–119.

Tiedje, J. M. (1988), *Ecology of Denitrification And Dissimilatory Nitrate Reductioni to Ammonium*, Wiley, New York.

Triska, F. J., V. C. Kennedy, R. J. Avanzino, G. W. Zellweger, and K. E. Bencala (1989), Retention and transport of nutrients in a 3rd-order stream—Channel processes, *Ecology*, *70*(6), 1877–1892.

Valett, H. M., J. A. Morrice, C. N. Dahm, and M. E. Campana (1996), Parent lithology, surface-groundwater exchange, and nitrate retention in headwater streams, *Limnol. Oceanogr.*, *41*(2), 333–345.

Vidon, P., C. Allan, D. Burns, T. P. Duval, N. Gurwick, S. Inamdar, S. Sebestyen (2010). Hot Spots and hot moments in riparian zones: Potential for improved water quality management 1, *J. Am. Water Resour. Assoc.*, *46*(2), 278–298, doi:10.1111/j.1752-1688.2010.00420.x.

Vidon, P. G. F., and A. R. Hill (2004a), Landscape controls on nitrate removal in stream riparian zones, *Water Resour. Res.*, *40*(3), W03201, doi:10.1029/2003WR002473.

Vidon, P. G. F., and A. R. Hill (2004b), Landscape controls on the hydrology of stream riparian zones, *J. Hydrol.*, *292*(1–4), 210–228, doi:10.1016/j.jhydrol.2004.01.005.

Whiting, P. J., and M. Pomeranets (1997), A numerical study of bank storage and its contribution to streamflow, *J. Hydrol.*, *202*(1–4), 121–136.

Zarnetske, J. P., R. Haggerty, S. M. Wondzell, and M. A. Baker (2011), Dynamics of nitrate production and removal as a function of residence time in the hyporheic zone, *J. Geophys. Res. Biogeosci.*, *116*, G01025.